Journal of Medicinal Chemistry

Article

Discovery of the Aryl-Phospho-Indole (IDX899), a highly potent anti-HIV non-nucleoside reverse transcriptase inhibitor

Cyril Dousson, François-René Alexandre, Agnès Amador, Séverine Bonaric, Stéphanie Bot, Catherine Caillet, Thierry Convard, Daniel da Costa, Marie-Pierre Lioure, Arlène Roland, Elodie Rosinovsky, Sébastien Maldonado, Christophe Parsy, Christophe Trochet, Richard Storer, Alistair Stewart, Jingyang Wang, BENJAMIN A MAYES, Chiara Musiu, Barbara Poddesu, Luana Vargiu, Michel Liuzzi, Adel Moussa, Jocelyn Jakubik, Luke Hubbard, Maria Seifer, and David Standring

J. Med. Chem., **Just Accepted Manuscript** • DOI: 10.1021/acs.jmedchem.5b01430 • Publication Date (Web): 23 Jan 2016

Just Accepted

ACS Publications

Journal of Medicinal Chemistry is published by the American Chemical Society. 1155 Sixteenth Street N.W., Washington, DC 20036

Discovery of the Aryl-Phospho-Indole (IDX899), a highly potent anti-HIV non-nucleoside reverse transcriptase inhibitor

Cyril Dousson[a‡], François-René Alexandre[a*‡], Agnès Amador[a,†], Séverine Bonaric[a,†], Stéphanie Bot[a], Catherine Caillet[a,†], Thierry Convard[a], Daniel da Costa[a], Marie-Pierre Lioure[a,†] , Arlène Roland[a,†], Elodie Rosinovsky[a,†], Sébastien Maldonado[a,†], Christophe Parsy[a], Christophe Trochet[a,†], Richard Storer[a,†], Alistair Stewart[b,†], Jingyang Wang[b,†], Benjamin A. Mayes[b,†], Chiara Musiu[b,†], Barbara Poddesu[b,†], Luana Vargiu[b,†], Michel Liuzzi[b,†], Adel Moussa[b,†], Jocelyn Jakubik[b,†], Luke Hubbard[b,†], Maria Seifer[b,†], David Standring[b,†]

[a]IDENIX, an MSD Company, 1682 rue de la Valsière, Cap Gamma, BP 50001, 34189 MONTPELLIER Cedex 4, France and [b]IDENIX, 320 Bent Street - 4th Floor, Cambridge, MA 02139, USA

[†]Former Idenix employees

ABSTRACT: Here, we describe the design, synthesis, biological evaluation and identification of a clinical candidate non-nucleoside reverse transcriptase inhibitors (NNRTIs) with a novel Aryl-Phospho-Indole (APhI) scaffold. NNRTIs are recommended components of highly active antiretroviral therapy (HAART) for the treatment of HIV-1. Since a major problem associated with NNRTI treatment is the emergence of drug resistant virus, this work focussed on optimization of the APhI against clinically relevant HIV-1 Y181C and K103N mutants and the Y181C/K103N double mutant. Optimization of the Phosphinate Aryl substituent led to the discovery of the 3-Me,5-Acrylonitrile-Phenyl analogue ***R$_P$*-13s** (IDX899) having an EC_{50} of 11 nM against the Y181C/K103N double mutant.

The reverse transcriptase (RT) of the human immunodeficiency virus type 1 (HIV-1) is a key enzyme in the replication cycle.[1] Inhibition of the HIV-1 RT leads to viral load declines in patients as shown with currently approved NNRTIs: nevirapine (NVP) **1**, efavirenz (EFV) **2**, delavirdine (DLV) **3**, etravirine (ETV) **4** and rilpivirine (RPV) **5**. NNRTIs bind to an allosteric hydrophobic pocket close to the polymerase active site of the HIV-RT, triggering a conformational change that inhibits the progression of viral DNA synthesis along the RNA template [2,3]. However, a single ami-

no acid mutation in the RT enzyme can lead to dramatic loss of efficacy of first generation NNRTIs such as NVP and EFV.[4,5,6] Clinically relevant mutants generated by first generation NNRTIs include Y181C, K103N and the Y181C/K103N double mutant (DM). The second generation NNRTI, etravirine, has an improved coverage of RT-mutants[7]. However, there is still a need for novel, chemically diverse, second generation NNRTIs with broader mutant coverage and an improved pharmaceutical profile[8,9,10].

Our goal in this work report was to develop a clinical candidate that retains good activity against the Y181C, K103N and Y181C/K103N mutants compared to EFV. The potency optimization of this series of APhI was performed using a cell-based HIV-1 assay to identify compounds that were potent enzyme inhibitors, and also had the ability to cross the cell membrane and inhibit the HIV-1 virus replication cycle in a living cell.

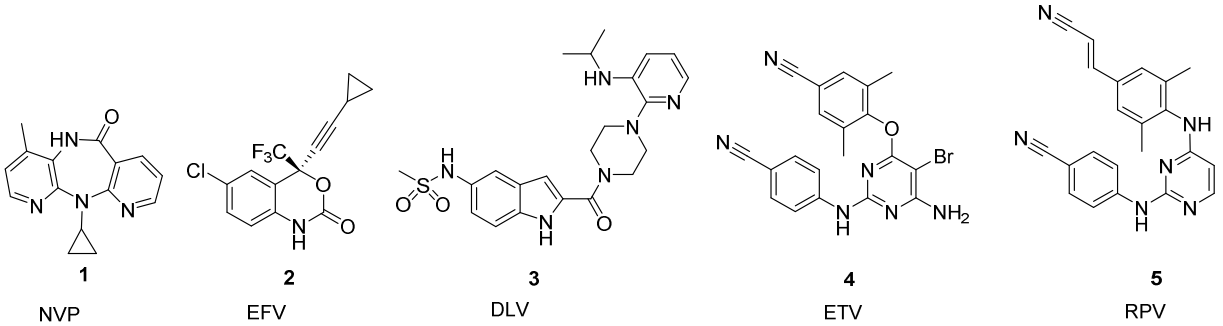

Figure 1. Marketed NNRTIs

In a previous communication[11a], we described the discovery of the APhI scaffold[11b-d]. A widely accepted strategy to improve the activity of an NNRTI against viruses containing the expected class resistant mutations is to build strong interactions of the drug with conserved regions of the NNI Binding Pocket (NNIBP)[12,13,14,15], such as highly conserved side chain residues or protein backbone atoms. Ideally, the candidate NNRTI should also demonstrate decreased interactions with mutable residues and exhibit some degree of conformational flexibility so that its binding can adapt to accommodate possible mutated amino acids[16]. Furthermore, it is known that in order to get robust potency, the ligand should have at least three points of interaction with the protein, and, ideally, these three points should not be aligned but form a triangle.

Based on reported structures (1FK9, 1FKO, 1JKH) of EFV, and other inhibitors[17] and the geometry requirements revealed by these structures, we postulated that:

- A substituted bicyclic scaffold that generates hydrogen bond interactions with backbone of K101 and lipophilic interactions or π/π interactions with F227.

- A branched tetrahedral linker could direct the substitution with the right angle towards the W229 conserved residue.

Phosphorus atom was selected as a key component of this linker because of its tetrahedral conformation, its novelty

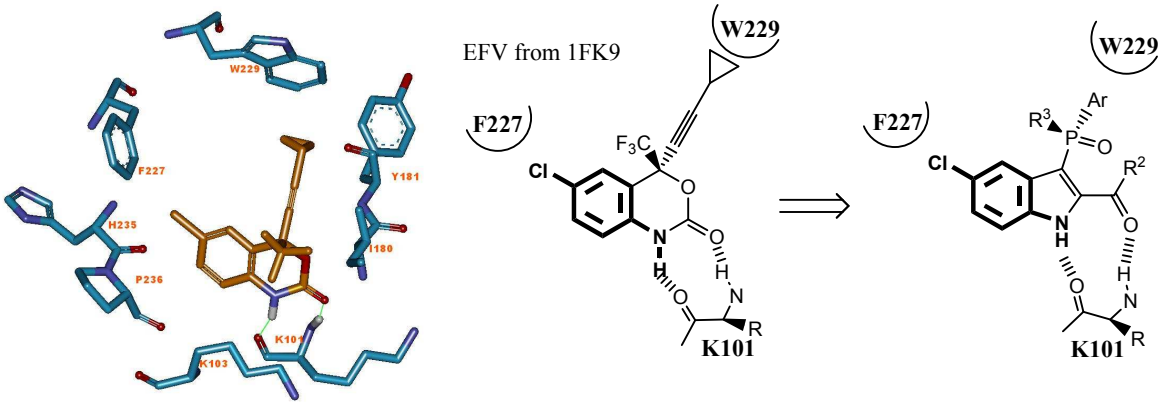

in this framework as well as for the opportunity of substitution allowed by its P^V oxidation state (Figure 2).

(a) (b) (c)

Figure 2. (a) X-ray of EFV in 1FK9 (some residues have been omitted for clarity). (b) Schematic view of EFV in 1FK9. (c) Selection of phospho-indole as novel scaffold.

In an earlier study we identified APhI **6** with the methyl phosphinate linker as lead series.[11a] The further optimization of this lead is described in the present report.

Chemistry

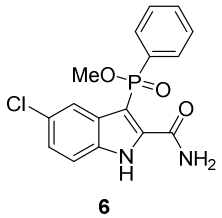

6

EC_{50} HIV-1 WT = 0.0007 μM

Figure 3. Lead APhI **6**

Two main synthesis strategies have been used to successfully give phospho-indole **13** with various substituents on the phosphorus (scheme 1 and 2), both started from key intermediate **7**[ub].

Scheme 1. Indole phosphinate synthesis – chlorophosphonate route

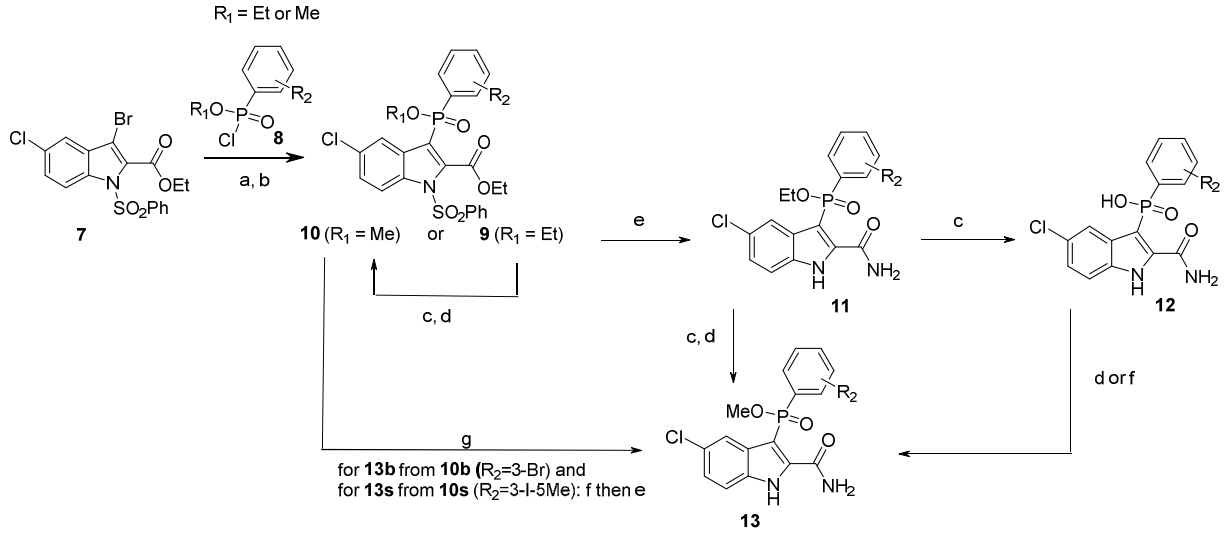

(a) n-BuLi, THF, -90 °C, 5 min; (b) **8** in THF, 20-80%; (c) TMSBr, DMF, 55 °C; (d) $P(OMe)_3$, 90 °C, 12-64%; (e) NH_3, MeOH, 50 °C, 13-77%; (f) $(Me)_3SiCHN_2$, MeOH, 5-27%; (g) $Pd(OAc)_2$, TlOAc, tri-o-tolylphosphine, acrylonitrile, DMF, µW, 110 °C, 2-56%.

Scheme 2. Indole phosphinate synthesis – indole H-phosphinate route

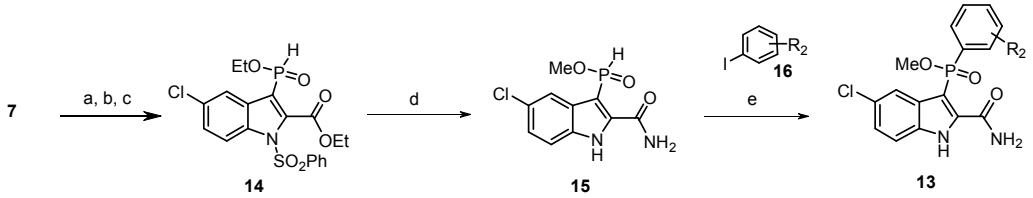

(a) n-BuLi, THF, -90 °C, 5 min; (b) Cl-$P(OEt)_2$; (c) HCl 0.5M/THF, 64% (3 steps); (d) NH_3, MeOH 50 °C, 42%; (e) **16**, $Pd(PPh_3)_4$, Et_3N, CH_3CN, µW, 85 °C, 8-10%.

The classical and linear chlorophosphonate route was first used as described previously[11a-c] for aromatic, heteroaromatic and alkyl R_2 substituents (Scheme 1) before more convergent indole H-ethyl-phosphinate **14** was developed (scheme 2). Attempts to directly give key intermediate indole H-Methyl phosphinate **15** succeeded by treatment with ammonia in methanol. Intermediate **14** was obtained from 3-bromo indole analogue *via* lithium-bromine exchange with *n*-BuLi at low temperature and nucleophilic substitution on chlorodiethylphosphite followed by indole-phosphonite acid monohydrolysis in 64 % overall yield. This route proved to be also generally useful for the preparation of APhI with different substitutions on the phenyl ring (compounds **13c** and **13t**).

Results and Discussion

During the course of this program, an extensive structure activity relationship (SAR) of the indole scaffold was conducted and more than 300 methyl phosphinate analogues were synthesized and evaluated in cellular assays using standard procedure. In this article we wish to report a focused SAR of 2-carboxamide,5-chloro indole phosphinates

and results are reported in Tables 1, 2, 3 and 4. The majority of the APhI synthesized were racemates at phosphorus and only a few selected compounds were resolved to test the two enantiomers. Cytotoxicities were evaluated during the course of the optimization of APhI and selectivity indexes proved to be over 1000 for most of the APhI (data not shown[11d]). Mono substituted phenyl phosphino-indoles were generally very potent against wild type HIV-1, but only those with long lipophilic groups tended to exhibit good activity against the mutant viruses as shown for compounds **13a** and **13b** (Table 1). The 3-*E*-acrylonitrile **13b** displayed single nanomolar potency on WT and the single mutants and, below 50 nM activity on the DM.

Table 1. Structure and Activity of APhI-carboxamides **6, 13a-13b**

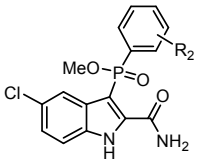

Compd	R_2	EC_{50} (μM)[a]			
		WT	K103N	Y181C	K103N/Y181C
EFV **2**		0.0007	0.037	0.0018	0.0580
6[11a]	H	0.0003	0.0100	0.0220	>1
13a	3-iPr	0.0005	0.0016	0.0084	0.0926
13b[b]	3-acrylonitrile (E)	0.0034	0.0032	0.0018	0.0495

[a]Primary MT-4 cell type assay. [b]Secondary MT-4 cell type assay.

Based on this result, other 3-substituted phenyl analogues with larger substituents were synthesized and tested. However, as shown in Table 2, 3-acrylonitrile (**13b**) was not sufficient to retain good activity against the DM when phenyl was substituted with 3-pyridine (**13c**). Furthermore, heterocycles such as 1-pyrazole or 2-thiophene (**13d**, **13e**), cycloalkyl (**13f**) or carboaromatics (**13g**) did not improve the DM activity.

Table 2. Structure and Activity of APhI-carboxamides **13c-13g**

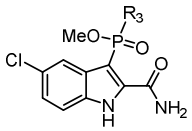

Compd	R_3	EC_{50} (μM)			
		WT	K103N	Y181C	K103N/Y181C

13c	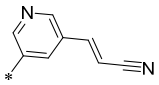	0.001	0.0025	0.0095	0.192
13d	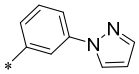	0.0045	0.059	0.1025	>1
13e	2-thiophene	0.0003	0.0034	0.0086	>1
13f	Cyclohexyl	0.0025	0.219	0.1008	>1
13g	1-naphtyl	0.0175	0.357	0.7272	>1

Phenyl substitutions on the phosphorus linker proved to have a significant influence on mutant activity. To further evaluate the effect of substituted phenyl groups on DM activity, we synthesized and tested di-substituted phenyl analogues as reported in Table 3. It appears that 3,5 disubstitution is better than 3,4 (**13h** *vs.* **13i**), which may be explained by the close proximity of W229 in the NNIBP. This steric requirement can also be observed when both methyls (**13i**) are replaced by fluorine (**13j**), chlorine (**13k**) or trifluoromethyl (**13l**), with the bulkier trifluoromethyl analogue giving the weakest activity. Further, it appears that fluorine may be too small to fulfill alkyl hydrophobic interactions with the P95 side chain of the protein, while methyl or chlorine substituents provided the best potency. The electronic density of the phenyl ring also played a role in the DM activity in this binding region; keeping the methyl/P95 interaction while modulating electronic density with small substituents led to the following ranking of activity against the DM: F>Cl>CN>Me>Br>OMe (**13i, 13m to 13q**). This ranking can be explained in part by π/π interactions (Figure 5) with the electron rich aromatic ring of the Y188 residue that lies stacked above the phenyl ring of the inhibitor; these π/π interactions become stronger with electron poor phenyl rings. This electronic requirement was further confirmed when comparing electron donating groups of **13t**, **13r** and the electron withdrawing acrylonitrile (**13s**), all having a similar length.

Compound **13t** proved to be the best WT inhibitor of this series displaying an exceptional EC_{50} value of 80 pM; however, it lost more than 1000-fold activity against the DM (EC_{50} = 111 nM). In contrast, compound **13s** exhibited the best DM activity and overall profile in the simple carboxamide series.

Table 3. Structure and Activity of APhI-carboxamides **13h-13t**

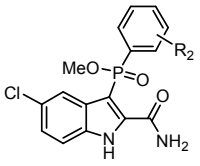

Compd	R_2	EC_{50} (μM)			
		WT	K103N	Y181C	K103N/Y181C
13h	3-Me-4-Me	0.0002	0.0229	0.0350	0.7920
13i	3-Me-5-Me	0.0010	0.0040	0.0150	0.2380
13j	3-F-5-F	0.0007	0.0065	0.0255	0.6420
13k	3-Cl-5-Cl	0.0003	0.0017	0.0199	0.2480
13l	3-CF_3-5-CF_3	0.0246	0.5268	0.9468	>1
13m	3-F-5-Me	0.0002	0.0005	0.0034	0.0690
13n	3-Cl-5-Me	0.0011	0.0056	0.0188	0.1141
13o	3-Br-5-Me	0.0030	0.006	0.0250	0.3685
13p	3-OMe-5-Me	0.0004	0.009	0.0230	0.663
13q	3-CN-5-Me	0.0010	0.0038	0.0184	0.1618
13r	3-$(CH_2)_2$CN-5-Me	0.0007	0.0007	0.0035	0.0285
13s	3-CH=CHCN-5-Me (*E*)	0.0029	0.0030	0.0030	0.0166
13t	3-OCH_2CN-5-Me	0.00008	0.0018	0.0087	0.1110

With compound **13s** exhibiting the best overall profile, its enantiomers were separated (***R*$_P$-13s** and ***S*$_P$-13s**) by chiral preparative HPLC. Consistent with the X-ray data, only the R_P enantiomer was active with a DM activity difference between the R_P and S_P enantiomers of over 110 fold. Compared to EFV, ***R*$_P$-13s** demonstrated over 30- and 4-fold better activity against the K103N and DM, respectively (Table 4 and Figure 4).

Table 4. Structure and Activity of enantiomers of **13s**

Compd	Structure	EC_{50} (μM)			
		WT	K103N	Y181C	K103N/Y181C
R_P-13s	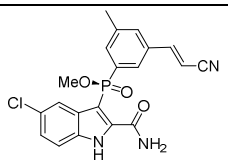	0.001	0.0013	0.0028	0.011

S_P-13s	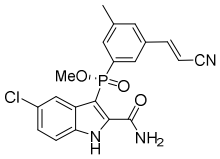	0.19	0.377	0.824	>1.25

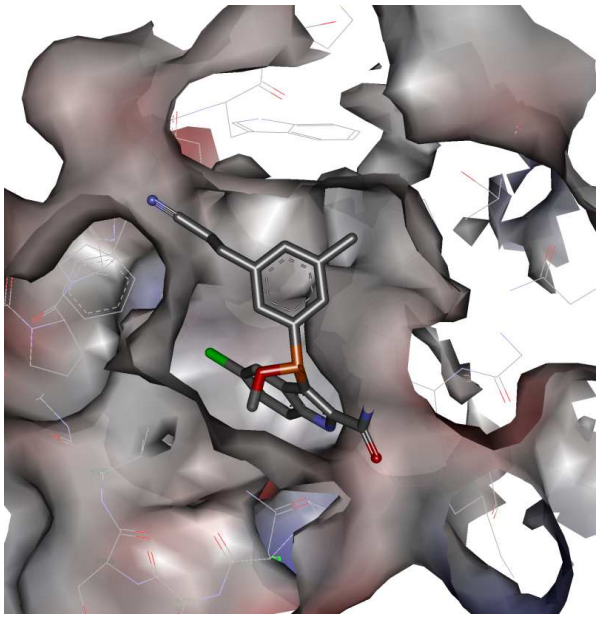

Figure 4. X-ray co-crystal top view of APhI ***R_P*-13s** (PDB 5FDL)

An X-ray structure of ***R_P*-13s** (Figure 4) bound to the NNIBP of HIV-RT DM was obtained at a resolution of 3.3 Å (PDB 5FDL). The corresponding ligand interaction diagram shows the residues interacting with the NNRTI (Figure 5).

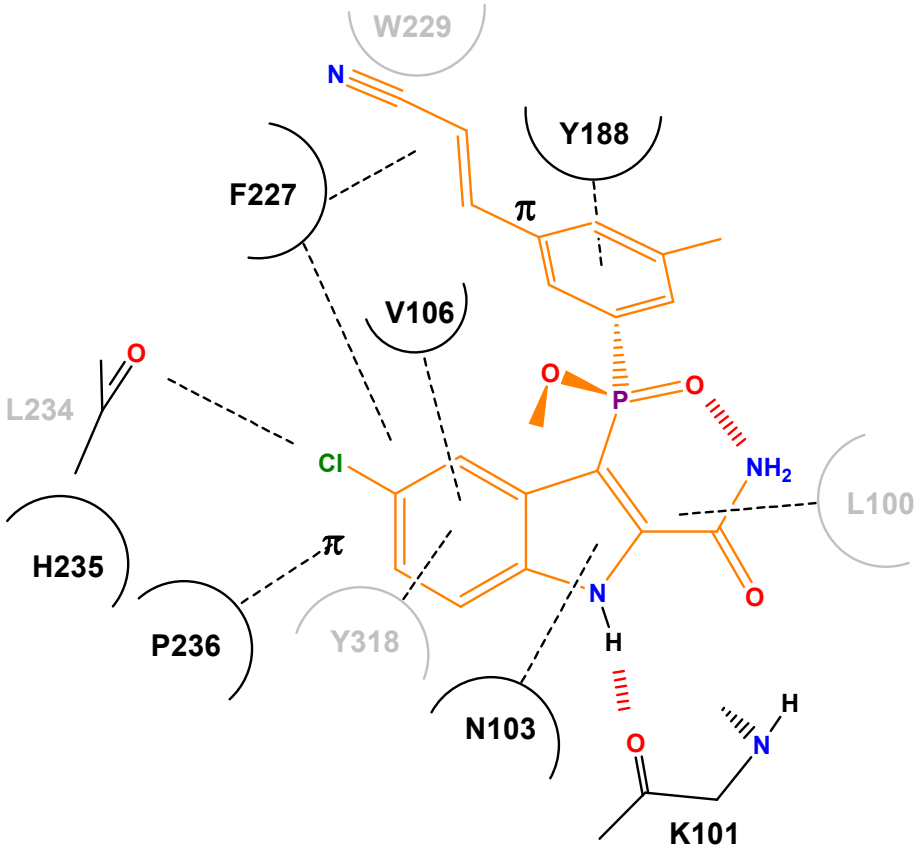

Style keys:Red large dashed line: hydrogen-bond interactions. Black dashed line: van der Waals, π and lipophilic interactions. Grey residues: positioned behind ***R*$_P$-13s**.

Figure 5. Ligand interaction diagram of ***R*$_P$-13s** with HIV-RT DM.

To further evaluate the drug potential of the APhI, the aqueous solubility of some analogues were determined. Compared to EFV (<0.5 μM), this series proved to be more soluble (Table 5). The bioavailability and pharmacokinetic profile were evaluated in three animal species (Table 6) and ***R*$_P$-13s** proved to have a good exposure in monkey when given orally as opposed to the low rat and dog AUC/dose values. ***R*$_P$-13s** *in vitro* data in hepatocytes (Table 7) suggest a better *in vivo* metabolic stability profile in human than the other species, with rat and dog giving the lowest values as previously observed *in vivo*. Given its excellent *in vitro* and *in vivo* profile, ***R*$_P$-13s** 5-chloro-3-[[3-[(E)-2-cyanovinyl]-5-methyl-phenyl]-(R)-methoxy-phosphoryl]-1H-indole-2-carboxamide (IDX899) was selected as a clinical candidate for human dosing[18].

Table 5. Solubility profile of APhIs

Compound	pH7.0 Aqueous solubility (μM)

EFV	<0.5
13a	0.8
13i	0.9
13m	1.7
R$_P$-13s	20

Table 6. PK profile of APhIs

Compound	Species [a]	Route [b]	Dose	Cmax (ng/mL)	Tmax (h)	$t_{1/2}$ (h)	AUC /Dose	Cl (mL/kg/h)	Vd (mL/kg)	F (%)
R$_P$-13s	Rat	IV	2.0	88.0	-	0.2	14.0	71.00	NC	-
	Rat	PO	10.0	25.0	0.4	5.9	5.0	-	NC	38.0
	Dog	IV	1.0	290.0	-	3.9	520.0	1.83	NC	-
	Dog	PO	5.0	18.0	1.5	2.4	22.0	-	NC	4.0
	Monkey	IV	1.0	1465.0	-	2.0	3026.0	0.33	NC	-
	Monkey	PO	5.0	945.0	3.0	3.1	1267.0	-	NC	42.0

[a] Mean PK Parameters (n=3 or 2)

[b] Vehicle : PEG400

Table 7. Metabolic stability in hepatocytes

	R$_P$-13s
Species	Parent cpd depletion: $t_{1/2}$ (min) [a]
Rat	17 ± 15
Dog	21 ± 10
Monkey	52 ± 24
Human	125 ± 55

[a] Independent experiments from 5 to 7 donors

Conclusion

We have successfully developed and optimized a new valuable NNRTI series, namely APhI, which proved to have substantial benefits in term of mutant activities, physicochemical properties and pharmacological profile. This work led to the discovery of ***R*$_P$-13s** (IDX899) as a new highly potent second generation NNRTI drug candidate. [19] Further to this work, ***R*$_P$-13s** progressed in phase IIb clinical trial where its development was suspended due to reports of seizures as part of a clinical trial involving treatment-experienced patients.[20]

Experimental Methods

Synthesis of Aryl Phospho Indoles. The synthesis of **(±)-13s** only is described here, while the synthesis of all other compounds is described in the Supporting Information.

All reactions were performed with reagent-grade materials under an atmosphere of nitrogen. Solvents were reagent-grade or better. Evaporation of the solvents was carried out in a rotary evaporator under reduced pressure. Thin layer chromatography (TLC) was performed on precoated aluminium sheets of silica gel 60 F254 (Merck, Art. 5554), visualization of products being accomplished by UV absorbance at 254 nm; column chromatography on silica 60 (40-63µm, Merck 11567). ^{1}H (400 MHz), ^{13}C (100 MHz) and ^{31}P (162 MHz) NMR spectra were recorded on a Brucker AC300 spectrometer using DMSO-d_6 or $CDCl_3$ as solvents. NMR chemical shift (δ) are quoted in parts per million (ppm) referenced to the residual solvent peak [DMSO-d_6] set at 2.49 ppm or [$CDCl_3$] set at 7.26 ppm. The accepted abbreviations are as followed: s, singulet; d, doublet; t, triplet; q, quartet; m, multiplet. Low-resolution LC mass spectra (LR LCMS) were recorded on a WATERS unit [Alliance 2695, Photodiode Array detector 2996, ZQ 2000 (ESCI source), Mass Lynx 4.1] using a reverse phase analytical column Synergy 4 µm Fusion 80A 50x2.0 mm (Phenomenex 100B-4424-BO). The compound to be analyzed was eluted using a linear gradient of 5% -95% acetonitrile in water with 0.05 % formic acid programmed over a 8 or 20 minutes period with a flow rate of 0.4 mL/min. Purity of all compounds was determined to be >95% by analytical HPLC using a WATERS unit [Alliance 2695, Photodiode Array detector 2996] using a reverse phase analytical column Waters Novapack C18 4µm 150x3.9 mm. The compound to be analyzed was eluted using a linear gradient of 5–95% acetonitrile over a 20 min period with a flow rate of 1 mL/min and the chromatogram was recorded using an UV detection from 210 to 400 nm (PDA Max Plot). Microwave assisted chemistry was performed with a CEM discover apparatus.

Ethyl 1-(benzenesulfonyl)-5-chloro-3-[(3-iodo-5-methyl-phenyl)-methoxy-phosphoryl] indole-2-carboxylate, **(±)-10s**: n-BuLi (2.5M in hexane, 2.17 mL, 5.42 mmol) was added dropwise to a stirred and cooled (to about -90 °C) solution of bromoindole **7** (2.0 g, 4.52 mmol) in anhydrous THF (45 mL) under nitrogen. After keeping the solution at about -90 °C for about 5 min, an appropriate chorophosphosphorus reagent **8s** (R_2=3-I,5-Me) (1.87 g, 5.42 mmol) was added dropwise to the solution at the same temperature. The reaction was allowed to warm up slowly to about -40°C (TLC monitoring, eluent CH_2Cl_2/EtOAc 9/1). Water (50 mL) was added and the reaction mixture was extracted with

EtOAc (3x 50 mL), dried and evaporated. The crude oil was purified by chromatography on silica gel to give **(±)-10s** (1.75 g, 49%) as a yellowish solid; ^{1}H NMR (DMSO-d_6, 300 MHz) δ (ppm) 1.40 (t, *J* = 7.12 Hz, 3H), 2.31 (s, 3H), 3.70 (d, *J* = 11.59 Hz, 3H), 4.46 (q, *J* = 7.12 Hz, 2H), 7.55 (dd, *J* = 2.13 Hz and *J* = 9.01 Hz, 1H), 7.61-7.72 (m, 3H), 7.79-7.91 (m, 4H), 8.06-8.12 (m, 3H); ^{31}P NMR (DMSO-d_6, 121.49 MHz) δ (ppm) 22.09; MS (ESI) m/z = 658.4 (MH^+).

5-chloro-3-[[3-[(E)-2-cyanovinyl]-5-methyl-phenyl]-methoxy-phosphoryl]-1H-indole-2-carboxamide **(±)-13s**: In a microwave tube, intermediate **(±)-10s** (0.467 g, 0.71 mmol) and acrylonitrile (17.75 mmol) in DMF (4.5 mL) were stirred at room temperature. This mixture was flushed few minutes with nitrogen. Tl(OAc) (0.187 g, 0.71 mmol), tri-o-tolylphosphine (0.086 g, 0.284 mmol) and $Pd(OAc)_2$ (0.037 g, 0.142 mmol) were added. The reaction mixture was heated under microwave irradiations under pressure at 110 °C (maximum power input 200 W) during 45 min. After concentration, the reaction mixture was purified by preparative HPLC to give the expected N-deprotected intermediate. ^{1}H NMR (DMSO-d_6, 300 MHz) δ (ppm) 1.11 (t, *J* = 7.07 Hz, 3H), 2.34 (s, 3H), 3.65 (d, *J* = 11.48 Hz, 3H), 4.14-4.25 (m, 2H), 6.5 (d, *J* = 16.69 Hz, 1H), 7.38-7.42 (m, 1H), 7.58-7.77 (m, 5H), 8.35-8.36 (m, 1H), 12.98 (brs, 1H); ^{31}P NMR (DMSO-d_6, 121.49 MHz) δ (ppm) 28.69; MS (ESI) m/z = 443.4 (MH^+). This compound was dissolved in methanol (10 mL) in a pressure tube and was stirred and cooled to 0°C. The solution was saturated with NH_3 gas for about 10 minutes. The mixture was stirred at about 50° C overnight, and after TLC monitoring, excess ammonia and methanol were evaporated in vacuo. The crude residue was purified by chromatography on silica gel column to give the expected carboxamide **(±)-13s** (0.164 g, 56%) as a white solid; ^{1}H NMR ($CDCl_3$, 300 MHz) δ (ppm) 2.36 (s, 3H), 3.85 (d, *J* = 11.7 Hz, 3H), 5.87 (d, *J* = 16.72 Hz, 1H), 6.20 (brs, 1H), 7.29-7.36 (m, 2H), 7.39 (brs, 1H), 7.53-7.66 (m, 4H), 10.97 (brs, 1H), 11.13 (brs, 1H); ^{31}P NMR ($CDCl_3$, 121.49 MHz) δ (ppm) 31.73; MS (ESI) m/z = 414 (MH^+).

HPLC chiral separation. Enantiomers of **(±)-13s** were separated by Supercritical Fluid Chromatography preparative method at Chiral Technologies. Preparative column: Chiralpak AD-H (250x20 mm) with CO_2/MeOH +1% diethylamine 80/20 as the mobile phase, flow rate 60 mL/min. Analytical column: Chiralcel OD-H (250x4.6 mm) with n-heptane/ethanol/diethylamine 70/30/0.1 as the mobile phase, flow rate 1.0mL/min. First eluting enantiomer ***R$_P$*-13s,** t_R=4.9 min, second eluting enantiomer ***S$_P$*-13s**, t_R=16.9 min, orders of elution refer to those observed on the preparative column.

HIV-1 infected cells inhibition experiments. The antiviral activity of compounds was measured by the inhibition of virus-induced cytopathogenicity in MT-4 cells using the HIV strain BH10 wild-type or the resistant viruses Y181C, K103N and Y181C/K103N as described in Hamann, M., Pierra, C., Sommadossi, J.P., Musiu, C., Vargiu, L., Liuzzi, M., Storer, R., and Gosselin, G. *Bioorg. Med. Chem.* **2009**, *17*, 2321-2326.

Pharmacokinetic profile of ***R$_P$*-13s** in rats, dogs and monkeys. Fed male Cynomolgus monkey, fed Beagle dogs and fasted Sprague Dawley rats were used. Dogs and monkeys were dosed at 1mg/kg intraveinous (IV) and 5 mg/kg orally (PO), rats at 5 mg/kg IV and 10 mg/kg PO, in a formulation of 10% dimethylacetamide/ 10% ethanol/ 80% PEG400. After dose administration, blood samples were collected from each animal predose and at 0.083, 0.25, 0.5, 1, 2, 3, 4, 8, 12 and 24 hours postdose *via* a femoral vein and transferred into tubes containing lithium-heparin anticoagulant. Plasma was spearated by centrifugation and stored at -70 °C until analysis. Concentration of unlabeled IDX899 within plasma samples were identified through high performance liquid chromatographics (HPLC) methods that incorporated tandem mass spectrometric detection (LC-MS/MS).

Supporting information. Synthetic procedure and characterization data of all compounds. This material is available free of charge via the internet at http://pubs.acs.org.

AUTHOR INFORMATION

Corresponding Author

* To whom correspondence should be addressed. Phone: +33(0)499522252; fax: +33(0)499522250. E-mail: francois-rene.alexandre@merck.com

Author Contributions

‡These authors contributed equally.

Notes

The authors declare no competing financial interest.

ACKNOWLEDGMENT

We thank Sareum Ltd (Cambridge, UK) Dr. P.M. Leonard, Dr. M. Fisher, Dr. M.B.AC. Lamers and Dr. J. Reader for X-ray structure determination of K103N/Y181C Mutant HIV-1 Reverse Transcriptase (RT) in Complex with the ligand (***R$_P$*-13s**).

ABBREVIATIONS

APhI, aryl-phospho-indole; DM, double mutant; EFV, efavirenz; ETV, etravirine; HAART, highly active antiretroviral therapy; HIV-1, human immunodeficiency virus type 1; NNIBP, nonnucleoside inhibitor-binding pocket; NNRTI, non-nucleoside reverse transcriptase inhibitor; NVP, nevirapine; PK, pharmacokinetic; RPV rilpivirine, RT, reverse transcriptase; WT, wild type.

Accession Codes

Crystal structure of K103N/Y181C Mutant HIV-1 Reverse Transcriptase (RT) in Complex with ***R*$_P$-13s** (IDX899) has been deposited in the RCSB Protein Data Bank under the PDB ID code 5FDL.

REFERENCES

[1] de Bethune, M.P. Non-nucleoside reverse transcriptase inhibitors (NNRTIs), their discovery, development, and use in the treatment of HIV-1 infection: A review of the last 20 years (1989–2009). *Antiviral Research* **2010**, 85, 75–90.

[2] Tantillo, C. ; Ding, J. ; Jacobo-Molina, A. ; Nanni, R. G.; Boyer, P. L. ; Hughes, S. H. ; Pauwels, R. ; Andries, K.; Janssen, P. A. J. ; Arnold, E. Locations of Anti-AIDS Drug Binding Sites and Resistance Mutations in the Three-dimensional Structure of HIV-1 Reverse Transcriptase. *J. Mol. Biol.* **1994**. *243*, 369-387.

[3] Ivetac, A.; McCammon, J. A. Elucidating the Inhibition Mechanism of HIV-1 Non-Nucleoside Reverse Transcriptase Inhibitors through Multicopy Molecular Dynamics Simulations. *J. Mol. Biol.*, **2009**, *388*, 644-658.

[4] Adkins, J. C.; Noble, S. Efavirenz. *Drugs*, **1998**, *56*, 1055-1064.

[5] Srivab, P.; Hannongbua, S. A study of the Binding Energies of Efavirenz to Wild-Type and K103N/Y181C HIV-1 Reverse Transcriptase Based on the ONIOM Method. *ChemMedChem*, **2008**, *3*, 803-811.

[6] Casado, J. L.; Moreno, A.; Hertogs, K.; Dronda, F.; Moreno, S. Extent and importance of cross-resistance to efavirenz after nevirapine failure. *AIDS Res. Hum. Retroviruses,* **2002**, *18*, 771-775.

[7] Andries, K. ; Azijn, H. ; Thielemans, T. ; Ludovici, D. ; Kukla, M.; Heeres, J.; Janssen, P.; De Corte, B.; Vingerhoets, J.; Pauwels, R.; De Bethune, M.-P. TMC125, a novel next-generation non-nucleoside reverse transcriptase inhibitor active against non-nucleoside reverse transcriptase inhibitor-resistant human immunodeficiency virus type 1. *Antimicrob. Agents Chemother.* **2004**, *48*, 4680-4686.

[8] Prajapati, D. G.; Ramajayam, R. ; Ram Yadav, M.; Giridhar, R. The search for potent, small molecule NNRTIs: A review. *Bioorg. Med. Chem.* **2009**, *17*, 5744-5762.

[9] Sweeney, Z. K.; Klumpp, K. Improving non-nucleoside reverse transcriptase inhibitors for first-line treatment of HIV infection: The development pipeline and recent clinical data. *Curr. Opin. Drug Discov. Devel.* **2008**, *11*, 458-470.

[10] Mehellou, Y.; De Clercq, E. Twenty-Six Years of Anti-HIV Drug Discovery : Where Do We Stand and Where Do We Go ? *J. Med. Chem.* **2010**, *53*, 521-538.

[11a] Alexandre, F.-R.; Amador, A.; Bot, S.; Caillet, C.; Convard, T.; Jakubik, J.; Musiu, C.; Poddesu B.; Vargiu L.; Liuzzi, M.; Roland, R.; Seifer M.; Standring D.; Storer, R.; Dousson, C.B. Synthesis and biological evaluation of Aryl-Phospho-Indole (API) as novel HIV-1 non-nucleoside reverse transcriptase inhibitors. *J. Med. Chem.,* **2011**, *54*, 392–395. [11b] Storer, R.; Dousson, C.B.; Alexandre, F.-R.; Roland, R.; Phospho-indoles as HIV inhibitors, *patent* US7,534,809B2, **2009**, May 19. [11c] Storer, R.; Dousson, C.B.; Alexandre, F.-R.; Roland, R.; Phospho-indoles as HIV inhibitors, *patent* US8,044,091B2, **2011,** October 25. [11d] Storer, R.; Alexandre, F.-R.; Dousson,

C.B.; Moussa A.M.; Bridges E.; Stewart A.; Wang J.Y.; Mayes B.A.; Enantiomerically pure phosphoindoles as HIV inhibitors, *patent* US7,960,428B2, **2011**, June 14.

[12] Hopkins, A. L. ; Ren, J. ; Milton, J. ; Hazen, R. J. ; Chan, J. H.; Stuart, D. L.; Stammers, D. K. Design of Non-Nucleoside Inhibitors of HIV-1 Reverse Transcriptase with Improved Drug Resistance Properties.1. *J. Med. Chem*. **2004**, *47*, 5912-5922.

[13] Zhan, P.; Liu, X.; Li, Z.; Pannecouque, C.; De Clercq, E. Design strategies of novel NNRTIs to overcome drug resistance. *Curr. Med. Chem*., **2009**, *16*, 3903-3917

[14] Paris, K. A.; Haq, O. ; Felts, A. K.; Das, K.; Arnold, E.; Levy, R. M. Conformational Landscape of the Human Immunodeficiency Virus Type 1 Reverse Transcriptase Non-Nucleoside Inhibitor Binding Pocket: Lessons for Inhibitor Design from a Cluster Analysis of Many Crystal Structures. *J. Med. Chem.*, **2009**, 52, 6413-6420.

[15] Ren, J.; Stammers, D. K. Structural basis for drug resistance mechanisms for non-nucleoside inhibitors of HIV reverse transcriptase. *Virus Res.*, **2008**, *134*, 157-170.

[16] Das, K. ; Clark, A. D. ; Lewi, P. J.; Heeres, J. ; De Jonge, M. R. ; Koymans, L. M. H. ; Vinkers, H. M.; Daeyaert, F. ; Ludovici, D. W.; Kukla, M. J.; De Corte, B. ; Kavash, R. W.; Ho, C. Y.; Ye, H.; Lichtenstein, M. A.; Andries, K.; Pauwels, R.; De Béthune, M.-P.; Boyer, P. L.; Clarck, P.; Hughes, S. H.; Janseen, P. A. J.; Arnold, E. Roles of Conformational and Positional Adaptability in Structure-Based Design of TMC125-R165335 (Etravirine) and Related Non-Nucleoside Reverse Transcriptase Inhibitors that are Highly Potent and Effective against Wild-Type and Drug-Resistant HIV-1 Variants. *J. Med. Chem*. **2004**, *47*, 2550-2560.

[17] Ragno, R. ; Frasca, S. ; Manetti, F. ; Brizzi, A.; Massa, S. HIV-Reverse Transcriptase Inhibition: Inclusion of Ligand-Induced Fit by Cross-Docking Studies. *J. Med. Chem*. **2005**, *48*, 200-212.

[18] Zhou, X. J.; Garner, R. C.; Nicholson, S.; Kissling, C. J.; Mayers, D. Microdose Pharmacokinetics of IDX899 and IDX989, Candidate HIV-1 Non-Nucleoside Reverse Transcriptase Inhibitors, Following Oral and Intravenous Administration in Healthy Male Subjects. *J. Clin. Pharmacol.* **2009**, *49*, 1408-1416.

[19] ***R$_P$*-13s** (IDX899) was evaluated in phase 2 clinical trial and was licensed to GlaxoSmithKline as of February 2009 and its name changed to fosdevirine/GSK2248761.

[20] Castellino,S.; Groseclose, M. R.; Sigafoos, J.; Wagner, D.; de Serres, M.; Polli, J. W.; Romach, E.; Myer, J.; Hamilton, B. Central Nervous System Disposition and Metabolism of Fosdevirine (GSK2248761), a Non-Nucleoside Reverse Transcriptase Inhibitor: An LC-MS and Matrix-Assisted Laser Desorption/Ionization Imaging MS Investigation into Central Nervous System Toxicity *Chem. Res. Toxicol.* **2013**, *26*, 241–251.

Table of Contents Graphic

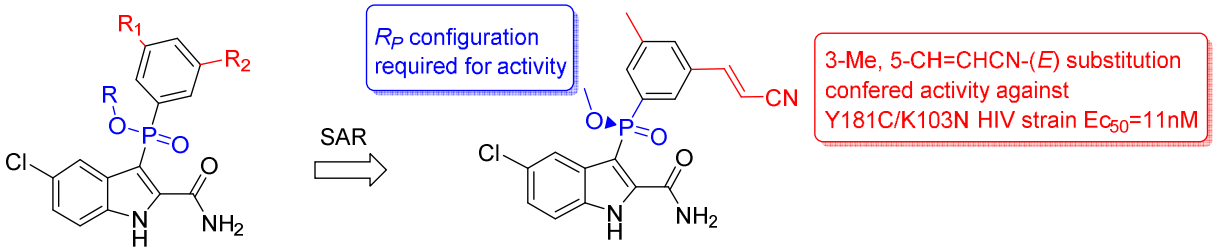
R1
R2
R
O
P
O
Cl
O
N
H
NH2
SAR
RP configuration required for activity
CN
3-Me, 5-CH=CHCN-(E) substitution confered activity against Y181C/K103N HIV strain Ec50=11nM

***R*$_P$-13s**